NASA TN D-1386

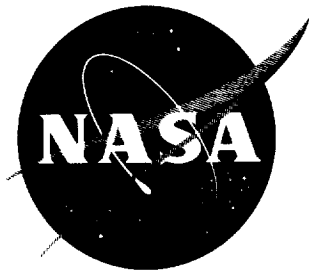

TECHNICAL NOTE

D-1386

EXPERIMENTAL INVESTIGATION OF THE EFFECTS OF COMPRESSIVE STRESS ON THE FLUTTER OF A CURVED PANEL AND A FLAT PANEL AT SUPERSONIC MACH NUMBERS

By Robert W. Hess and Frederick W. Gibson

Langley Research Center
Langley Station, Hampton, Va.

NATIONAL AERONAUTICS AND SPACE ADMINISTRATION
WASHINGTON
October 1962

NATIONAL AERONAUTICS AND SPACE ADMINISTRATION

TECHNICAL NOTE D-1386

EXPERIMENTAL INVESTIGATION OF THE EFFECTS OF COMPRESSIVE STRESS ON THE FLUTTER OF A CURVED PANEL AND A FLAT PANEL AT SUPERSONIC MACH NUMBERS

By Robert W. Hess and Frederick W. Gibson

SUMMARY

An investigation was made of the effects of compressive stress on the flutter of a curved and a flat panel. The curved panel which was 0.0075-inch-thick stainless steel with a length-width ratio of 2.13 and a radius-to-thickness ratio of 1,133 was tested at a Mach number of 1.97. A flat aluminum panel, 0.032 inch thick with a length-width ratio of 2.13, was tested at Mach numbers of 1.63 to 1.84.

The dynamic pressure at flutter decreased with increased axial compressive stress to a point where the panel was loaded to a stress near the calculated critical buckling stress. Beyond this point, the dynamic pressure at flutter increased with increasing compressive stress. The results of the flat-panel flutter tests indicate that caution should be exercised in using existing empirical panel flutter boundaries.

INTRODUCTION

A large amount of flat-panel flutter data has been obtained by various investigators (see, for instance, refs. 1 and 2), and a panel flutter boundary based on these data has been established. The parameter used to define this boundary is a nondimensional ratio of panel stiffness to aerodynamic stiffness and this parameter varies with panel length-width ratio. This parameter omits many factors that are known to affect panel flutter such as midplane stresses, edge conditions, pressure differential, and curvature. Of particular interest to space vehicle designers are the effects on the panel flutter boundary of curvature and midplane stresses. Very little curved panel data are available and it would be advantageous if the flutter characteristics of curved panels could be related to the existing flat-panel flutter data.

This paper presents the results of tests on both flat and curved panels mechanically loaded in compression that demonstrate the effect of

midplane stresses on panel flutter and relate them to the calculated panel critical buckling stress. Also, a method is suggested for estimating the effect of curvature on the flutter of axially compressed panels.

The results were obtained on a curved steel panel tested in the Langley 9- by 18-inch supersonic aeroelasticity tunnel at a Mach number of 1.97 and a flat aluminum panel tested in the Langley Unitary Plan wind tunnel at Mach numbers of 1.63 and 1.84.

SYMBOLS

a	speed of sound
B	panel flutter parameter $\left(\frac{\beta E}{q}\right)^{1/3} \frac{t}{l}$
$D = \frac{Et^3}{12(1 - \nu^2)}$	
E	elastic modulus
f	flutter frequency
G	shear modulus
l	panel length
M	Mach number
p	pressure
Δp	pressure difference across panel skin, positive for pressure in cavity behind panel greater than free stream
q	dynamic pressure
r	radius
T	temperature
t	panel thickness
w	developed panel width

w_b panel width between stiffener center lines

$\beta = \sqrt{M^2 - 1}$

ρ air density

ν Poisson's ratio

σ stress

σ_{cr} critical buckling stress

Subscripts:

c cylinder

f flat plate

p panel

0 total conditions

1,2 position on panel

MODELS

Curved Panel

The model, of 0.0075-inch-thick stainless steel with a radius-to-thickness ratio of 1,133 and a length-width ratio of 2.13 per bay, was a section of an elliptically shaped cylinder composed of four circular arcs. This cross section was chosen to approximate the restraints on a three-bay longitudinally stiffened cylindrical shell while maintaining representative curvature within tunnel-size limitations. The portion of the cylinder exposed to the airstream (figs. 1 and 2) was divided into three bays (fig. 1) by 0.019-inch-thick stainless-steel stiffeners welded to the skin. The arc length between the stiffener center lines was 3.4 inches and the length of the panel between doublers was 7.25 inches. The radius of the section of the cylinder exposed to the airstream was designed to be 1 foot. However, because of stresses imposed in the process of fabrication, the radius of each individual bay was 8.5 inches and this dimension was used in the calculations. The decrease in the radius became apparent after the stiffeners and doublers were welded to the skin. The material properties of the skin and longitudinal stiffeners used in the calculations are given in table I.

Angle rims (figs. 3 and 5) were attached with screws to the leading and trailing edges of the model and steel bulkheads were in turn bolted to these rims. The model was attached at the leading edge to a tunnel sidewall plate by a pair of brackets which were bolted to the leading-edge bulkhead and the tunnel sidewall plate. (See figs. 4 and 5.)

The model was loaded at the trailing edge by means of a compression screw jacked against a strain-gaged load cell. The load cell was suspended between the trailing-edge bulkhead and the compression screw by ball and socket joints. A short cylindrical housing enclosed the back of the assembly and sealed it off from atmospheric pressures. The pressure differential across the panel was regulated by venting the back of the housing through a 2.5-inch pipe to a 2.5-inch vent in the tunnel sidewall opposite the panel. A 5° ramp was positioned in front of the vent to give a minimum pressure differential across the panel. Leading- and trailing-edge cone-cylinder fairings (fig. 2) were attached to the tunnel sidewall; the fairings had semivertex angles of 5° and 9°, respectively.

Flat Panel

As is shown in figures 6 to 8, the 0.032-inch-thick aluminum panel was divided into nine bays by two external longitudinal hat-section stiffeners and two internal lateral frames. A Z-stiffener was riveted to the skin at each side and end of the panel. The center bay panel with a length-width ratio of 2.13 was the test model; the other eight bays served to provide the elastic restraint. The test panel was 6.9 inches wide and 14.68 inches long measured from rivet line to rivet line. The material properties of the panel are given in table I.

The model was mounted on a splitter plate as shown in figures 6 and 9. External steel clamping straps were bolted at 1-inch centers to all edges of the panel. Axial load was applied by jacking compression screws against solid blocks which were attached to the external longitudinal stiffeners at the trailing edge. Similar blocks were attached to the stiffeners at the leading edge to resist the load. The cavity in the splitter plate was vented to a vacuum line to control the pressure difference across the panel.

Two sets of fairings (fig. 9) were used with this model. On all but the last run, fairings were attached to the splitter plate ahead of each external stiffener. A wedge was placed in front of the model (fig. 10) for the last run to determine the effects of a separated flow on the flutter of the panel.

INSTRUMENTATION

Curved Panel

A continuous record was made during each run of the outputs of the load cell, stagnation pressure, and temperature transducers on a recording oscillograph. The signal from the load cell was also read on an automatic null balance indicator. Signals from four deflectometers (variable reluctance pickups) and three strain gages were also recorded and were used to determine the onset of flutter and the flutter frequency. Motion pictures were taken at 1,000 frames per second to study the motion of the panel.

Flat Panel

Compression and bending stress, panel temperature and frequency, and tunnel conditions were measured during each test. As may be seen in figures 7 and 8, five sets of strain gages measuring compressive stress, three sets of strain gages measuring bending stress, and two thermocouples were mounted on each panel. One set of compression gages was mounted at the trailing edge of the center bay panel and two were mounted on each stiffener between the lateral frames and the ends of the stiffener. Two deflectometors were used to monitor the frequencies of the center bay panel. One of the three bending gages was mounted at the trailing edge of the center bay panel and one on each stiffener. The signals from the five compression gages, the two thermocouples, and the pressure cells measuring stagnation pressure and pressure differential were obtained directly from automatic null balance indicators. A continuous tape recording was made during each run of the signals from the bending gages and two deflectometers. These signals were also monitored on a recording oscillograph. Motion pictures were taken at 1,000 frames per second at each flutter point to study the motion of the panel.

TEST PROCEDURES

Curved Panels

The panels were tested in the Langley 9- by 18-inch supersonic aeroelasticity tunnel at a Mach number of 1.97. The panels were loaded by slowly jacking the compression bolt against the load cell until the number of counts on the automatic null balance indicator corresponded to a preselected load. The tests were run by gradually increasing the dynamic pressure until flutter started, or until maximum tunnel dynamic pressure was reached, after which the test was terminated. The pressure differential across the center bay panel was less than 0.1 pound per square inch for all tests.

Flat Panel

The test was conducted in the low Mach number section of the Langley Unitary Plan wind tunnel at Mach numbers of 1.63 and 1.84. Before each test the clamping straps were loosened along the two sides and at the trailing edge and a compressive force was applied by jacking the compression bolts against the blocks at the trailing edge of the two external longitudinal stiffeners. The load was applied in increments to keep the indicated average stiffener stress of compression gages 1 and 3 the same as that of compression gages 2 and 4. The clamping straps were tightened when the desired average stresses in the two stiffeners was the same. This clamping caused a noticeable change in the average stress of the two stiffeners.

The minimum flutter dynamic pressure was determined by using the following method. The pressure differential across the panel was varied, approximately ±30 pounds per square foot, as the dynamic pressure was slowly increased until the center bay panel fluttered. Then, the pressure differential was varied and the amplitudes of the deflectometers and bending gages were monitored on the oscilloscope to determine the pressure differential at maximum amplitude response. With this pressure differential held, the dynamic pressure was then decreased until flutter stopped. At this point the dynamic pressure was again slowly increased with the panel subject to the same pressure differential until the panel fluttered again. This process was repeated a sufficient number of times to ensure determination of the minimum flutter dynamic pressure for each preload setting.

RESULTS AND DISCUSSION

Curved Panel

The test results are presented in table II and in figure 11. The table lists the tunnel conditions at flutter (or the maximum tunnel conditions at no flutter), the flutter frequency, the compressive load, and the compressive stress which was determined by dividing the compressive load by the cross-sectional area of the skin and stiffener. The value of the panel flutter parameter $\left(\frac{\beta E}{q}\right)^{1/3}\frac{t}{l}$ is also listed for each run. The adjusted panel flutter parameter, which is discussed later in the paper, is also given.

The results of the tests are presented in figure 11 on a plot of the dynamic pressure at the start of flutter as a function of the compressive stress. The dynamic pressure at flutter decreases with

increasing compressive stress to a minimum beyond which the dynamic pressure increases with increasing stress. The dynamic pressure at the test point at which no flutter occurred (indicated by the solid symbol in fig. 11) was three times greater than the dynamic pressure of the minimum flutter q test point. The compressive stress at this minimum point is noted to be near the value of the calculated critical buckling stress which is indicated on the abscissa. The critical buckling stress was calculated from the Redshaw equation (ref. 3, eq. 8.4):

$$\left(\frac{\sigma_{cr}}{E}\right)_p = \sqrt{\left(\frac{\sigma_{cr}}{E}\right)_c^2 + \frac{1}{4}\left(\frac{\sigma_{cr}}{E}\right)_f^2} + \frac{1}{2}\left(\frac{\sigma_{cr}}{E}\right)_f \tag{1}$$

where

$$\left(\frac{\sigma_{cr}}{E}\right)_c = 9\left(\frac{t}{r}\right)^{1.6} + 0.16\left(\frac{t}{l}\right)^{1.3} \tag{2}$$

is Kanemitsu and Nojima's empirical equation for the critical buckling stress of a cylinder and

$$\left(\frac{\sigma_{cr}}{E}\right)_f = K\,\frac{\pi^2 E}{12\left(1 - \nu^2\right)}\left(\frac{t}{w_b}\right)^2 \tag{3}$$

is Bryan's flat-plate equation. The coefficient K is a function of the length-width ratio and the ratio of panel bending stiffness to the torsional rigidity of the edge support and was obtained from figure 5.9 in reference 3. Equation (1) gives a conservative estimate of the critical buckling stress which is compatible with the fact that distortions, as discussed previously, were imposed during the construction of the panel. The alinement of the critical buckling stress and the minimum flutter point may not be a general result since analytical results in reference 4 indicate that the minimum dynamic pressure at flutter may occur at a ratio of σ/σ_{cr} that is a function of the length-width ratio.

Flat Panel

The results of the tests are presented in table III and in figure 12. The table lists the tunnel conditions at flutter, the flutter frequency, the compression and bending stresses, the temperatures at the two thermocouple locations, and $\left(\frac{\beta E}{q}\right)^{1/3}\frac{t}{l}$, the panel flutter parameter. Data that were obtained at the start of flutter and data obtained at a dynamic

pressure higher than that at the start of flutter are listed under comments in table III as minimum flutter q and maximum flutter q, respectively.

As may be noted in the tabulation of static stress in table III, there was a considerable stress gradient along the longitudinal axis of the panel as evidenced by the difference in the compressive stress at the two points on each stiffener. The compressive stress at the point near the trailing edge was higher than the stress near the leading edge by as much as a factor of seven. This difference was due in most part to the fact that part of the load applied at the trailing edge of the hat stiffeners was carried by the side panels and Z-stiffeners. It should also be noted that there was a shift in the stress between the clamped no-wind stress and the stress at each flutter point. This realinement of stress may be due to the forces, on the unevenly loaded panel, from the mild starting shock, and forces generated in the process of determining the minimum flutter q. It is also possible that this change in stress may be due in part to the slight increase in panel temperature from room temperature.

The results of the tests are plotted in figure 12 for the minimum dynamic pressure at flutter as a function of the compressive stress at the trailing edge of the center bay panel for both Mach numbers. The values of stress assigned to the flagged symbols (for which no panel stress data were obtained) was estimated by assuming the ratio of the average panel stress to average stiffener stress to be approximately constant. The value of the critical buckling stress used in figure 12 was calculated from equation (3).

The flat-panel flutter data in figure 12 exhibit a trend similar to that of the curved-panel flutter data of figure 11. The dynamic pressure at flutter increases with increasing compressive panel stress when the panel is loaded beyond the calculated critical buckling stress. The lowest dynamic pressure at flutter (M = 1.63) in this test occurred when the panel was loaded to a point near the calculated critical buckling stress and was approximately one-sixth the dynamic pressure of the no-flutter point (M = 1.63) when the panel was in an unstressed condition. However, this q may not be the minimum flutter q of the panel at M = 1.63 since there were not enough data to define a curve.

A noticeable trend observed during the flutter tests was that, once flutter was initiated, the panel continued to flutter at dynamic pressures below the minimum starting flutter q. For example, the minimum dynamic pressure at the start of flutter for run 4 point 1 was 624.5 pounds per square foot but, after the panel locked into flutter, it was possible (at the same Δp) to decrease the dynamic pressure to 565 pounds per square foot before flutter stopped. Similarly, the minimum dynamic pressure at flutter for run 7, point 1 was 1,292 pounds

per square foot, but flutter stopped at a dynamic pressure of 1,130 pounds per square foot. Thus a panel can flutter over a longer length of time than may be indicated by a flutter boundary and a proposed trajectory.

No change was made in the compression bolt settings between the end of run 6 and the beginning of run 7 (when the stiffener fairings were replaced by the wedge) and the two runs should serve to give a direct comparison between the two flow conditions. However, the data in table III show that the compression stress in run 7, as indicated by the two remaining strain gages, to be lower than that for run 6. At flutter the forward panels bulged out noticeably into the airstream, as might be expected, because of the low pressure area behind the wedge. The minimum dynamic pressure at flutter for run 6 was 773 pounds per square foot while the minimum at flutter was 1,292 pounds per square foot for run 7.

Fatigue cracks at the trailing edge of the center bay panel were not discovered until the end of the last run. This damage was the result of at least 29 minutes of flutter. It was also noted that deflectometer coils interfered with the motion of the panel as was evidenced by slight impressions of the coil in the panel. The coils were 1/4 inch behind the panel.

Comparison With Other Data

Flat panels.- The flutter boundaries in references 1 and 2 were empirically determined and have been used in estimating the minimum panel thickness necessary to prevent flutter. However, the results of the flat-panel tests reported in this paper and other data published in recent papers indicate that these boundaries are unconservative for elastically restrained panels loaded in compression.

The results of the present tests and recently published data are presented in figure 13 in terms of the panel flutter parameter $\left(\frac{\beta E}{q}\right)^{1/3}\frac{t}{l}$, as a function of the length-width ratio. Most of the panels fluttered at a dynamic pressure that was lower than that indicated by the flutter boundary of reference 2 or required a greater thickness to prevent flutter. The spread in the flutter data of references 5 and 6 is due to variations in thermal stress. The flat aluminum panels of reference 3 had four bays and were subjected to pressure differentials of ± 0.5 pound per square inch. The panel flutter results from reference 6 are from the flat Inconel-X panels located forward of the main spar of the X-15 ventral fin. The variation of the data from reference 7 is due to changes in cavity

depth behind a fiberglass, foam-laminated panel when the pressure differential was nearly 0.

As may be noted in figure 13, data from each group of tests, with the exception of the curved-panel data, exceed the flutter boundary from reference 2 over a large range of l/w. It is also interesting to note that these panels, with the exception of those of reference 7, were part of built-up structures with multiple bays and, as such, the test panels were subject to elastic edge restraints. It appears that there are now sufficient data, over a large range of l/w, to consider a design curve that will give more conservative values of the flutter parameter for panels near the critical buckling stress. Such a curve is incorporated in figure 13 as a solid line.

Effects of curvature.- One reason that the curved-panel flutter data fall well below the curves in figure 13 is that the additional stiffness due to curvature is not accounted for in the flutter parameter. Since the critical buckling stress was observed to be an important factor in both flat and curved panels, an adjusted thickness was obtained by determining the thickness of a flat plate, having the l/w and edge restraint of the curved panel and the same calculated critical buckling stress of the curved panel. Figure 14 shows the curved-panel data for which both the actual thickness (0.0075 inch) and the adjusted thickness (0.0173 inch) have been used in computing the flutter parameter. The use of the adjusted thickness in the panel flutter parameter brings the data up to the curve and may prove to be a useful device in estimating the effects of curvature on the flutter of axially compressed curved panels.

CONCLUDING REMARKS

The results of preliminary flutter tests on a flat and a curved panel (with length-width ratios of 2.13) indicate that the compressive stress in the panel has a large effect on the dynamic pressure at flutter in that the dynamic pressure at flutter appears to be a minimum when the panel is near its critical buckling stress.

The results of the flat-panel flutter tests and other recent data indicate that previously published panel flutter boundaries may be unconservative for panels with axial compressive stresses near the critical value.

The curved-panel results indicate that the use of an adjusted thickness in the panel flutter parameter may prove to be useful in estimating the effects of curvature on the flutter of axially compressed panels.

Extensive tests over a wide range of length-width ratios, panel curvature, and compressive stress are necessary for a more complete understanding of the effects of these variables on panel flutter.

Langley Research Center,
National Aeronautics and Space Administration,
Langley Station, Hampton, Va., June 8, 1962.

REFERENCES

1. Sylvester, Maurice A.: Experimental Studies of Flutter of Buckled Rectangular Panels at Mach Numbers From 1.2 to 3.0 Including Effects of Pressure Differential and of Panel Width-Length Ratio. NASA TN D-833, 1961.

2. Kordes, Eldon E., Tuovila, Weimer J., and Guy, Lawrence D.: Flutter Research on Skin Panels. NASA TN D-451, 1960.

3. Sechler, Ernest E., and Dunn, Louis G.: Airplane Structural Analysis and Design. John Wiley & Sons, Inc., 1942.

4. Leonard, Robert W., and Hedgepeth, John M.: Status of Flutter of Flat and Curved Panels. NACA RM L57D24c, 1957.

5. Dixon, Sidney C., Griffith, George E., and Bohon, Herman L.: Experimental Investigation at Mach Number 3.0 of the Effects of Thermal Stress and Buckling on the Flutter of Four-Bay Aluminum Alloy Panels With Length-Width Ratios of 10. NASA TN D-921, 1961.

6. Bohon, Herman L.: Panel Flutter Tests on Full-Scale X-15 Lower Vertical Stabilizer at Mach Number of 3.0. NASA TN D-1385, 1962.

7. Tuovila, W. J., and Presnell, John G., Jr.: Supersonic Panel Flutter Test Results for Flat Fiber-Glass Sandwich Panels With Foamed Cores. NASA TN D-827, 1961.

TABLE I.- MATERIAL PROPERTIES OF PANELS

	Flat panel (aluminum)		Curved panel (stainless steel)	
	Skin	Stiffener	Skin	Stiffener
E, psi	10.7×10^6	10.3×10^6	27×10^6	26×10^6
ν, in./in.	0.338		0.227	
G, psi		3.9×10^6		11.5×10^6
D, in-lb	30.2		1.002	
t, in.	0.032	0.050	0.0075	0.019

TABLE II.- CURVED-PANEL TEST RESULTS

[M = 1.97]

Run	q, psf	p_0, psia	ρ, slugs/cu ft	T_0, °R	a, fps	Compressive load, lb	Compressive stress, psi	f	B	B, adjusted
*1	2,096	40.0	14.25×10^{-4}	552	865	1,348	3,180	---	0.151	0.230
2	958	18.3	6.41	561	872	1,636	3,859	185	.196	.452
3	964	18.4	6.55	552	865	1,596	3,765	200	.195	.450
4	1,022	19.5	6.9	556	868	1,580	3,727	142	.178	.410
5	950	18.1	6.41	556	868	1,520	3,586	137	.196	.452
6	1,083	20.7	7.27	559	870	1,500	3,539	140	.188	.434
7	776	14.8	5.28	551	864	1,649	3,890	145	.210	.484
8	860	16.4	5.82	554	866	1,678	3,958	100	.203	.468
9	698	13.3	4.74	552	865	1,720	4,058	85	.218	.503
10	798	15.2	5.40	552	865	1,762	4,157	86	.208	.480
11	738	14.1	5.03	550	863	1,638	3,864	100	.214	.493
12	727	13.9	4.94	552	865	1,784	4,208	100	.215	.496
13	744	14.2	5.05	553	865	1,766	4,166	100	.213	.491
14	846	16.1	5.72	555	868	1,820	4,293	110	.204	.470
15	722	13.8	4.88	555	868	1,815	4,282	100	.215	.496
16	782	14.9	5.26	557	869	1,857	4,367	118	.210	.484
17	1,027	19.5	6.95	552	865	1,862	4,392	105	.192	.443

*No flutter point.

TABLE III.- FLAT-PANEL TEST RESULTS

[The stagnation temperature was 585° R for all tests. The speed of sound was 958 ft/sec for M = 1.63; the speed of sound was 916 ft/sec for M = 1.84.]

Run	Point	M	q, lb/sq ft	p_0, lb/sq ft	Δp, lb/sq in.	ρ, slug/cu ft	B	f, cps	Compressive stress from gages - 1	2	3	4	5	Bending stress (1/2 peak to peak) from gages - 6	7	8	T_1, °F	T_2, °F	Comments
1	1	1.63	1,250	3,000	0.198	10.28×10^{-4}											99	102	No flutter. No load on panel.
2	(a)								752	3,480	9,700	9,140	1,030						
	1	1.63	441.5	1,058	-0.308	3.63	0.360	133	2,241	3,684	9,760	10,227	1,221	112.5	1,530	236.4	90	94	Minimum flutter q.
	2	1.84	442	1,087	-.111	2.970	.388	137	1,980	3,280	9,049	9,266	1,348		1,530		87	92	Maximum flutter q obtained during run.
	3	1.84	314.5	800	-.103	2.185	.428	140	2,146	3,495	9,369	9,457	1,593		1,462		87	93	Minimum flutter q.
3	(a)								1,488	2,140	6,350	6,450	897				89	93	
	1	1.63	410	984	-0.231	3.375	0.369	140	911	1,688	8,881	9,075	1,276	93.7	925	118	92	97	Minimum flutter q.
	2	1.84	349	899	-.109	2.46	.413	140	2,190	2,800	8,710	8,660	[b]1,243						Minimum flutter q.
4	(a)								2,510	3,810	13,550	13,700	2,210						
	1	1.63	624.5	1.497	-0.127	5.115	0.320	212	1,584	2,170	14,165	17,667	1,745		(c)		(c)	97	Mimimum flutter q. Panel fluttered approximately 6 minutes at varying q and Δp.
	2	1.84	772	1,988	.049	5.435	.317	180	1,592	1,610	11,707	11,544	[b]1,471		(c)		(c)	97	Minimum flutter q. Could not stop flutter with a Δp of 0.48 psi.
5	(a)								1,250	955	5,190	5,250							
	1	1.63	210.8	505	-0.159	1.733	0.461	145	1,362	1,657	7,589	7,257	[b]993		(c)		(c)	102	Minimum flutter q.
	2	1.63	713	1,709	-.118	5.86	.307	145	839	655	5,746	5,518	(c)		(c)		(c)	102	
	3	1.63	834	2,001	-.310	6.88	.291	180	958	1,002	7,374	7,098	(c)		(c)		(c)	105	5 minutes of flutter at this point.
	4	1.63	1,251	3,003	-.288	10.30	.254	211	634	339	6,184	5,994	(c)		(c)		(c)	110	10 minutes of flutter while increasing q from point 3 to point 4.
6	(a)								3,200	5,500	21,550	21,300	(c)		(c)		(c)		
	1	1.63	773	1,853	-0.166	6.36	0.298	233	2,518	2,548	21,107	23,121	(c)		(c)		(c)	99	Could not use Δp to stop flutter.
7	(a)								3,200	5,500			(c)		(c)		(c)		
	1	1.63	1,292	3,099	0.187	10.630	0.251	203	1,647	1,688	(c)	(c)	(c)		(c)		(c)	(c)	Minimum flutter q.
	2	1.63	2,080	4,980		17.080	.215	209					(c)		(c)		(c)		Maximum flutter q obtained during run. Approximately 8 minutes of flutter going from q of 1,292 psf to a q of 2,080 psf.

[a]Screws tight on clamp, no air flow.

[b]Estimated values.

[c]No signal from transducer.

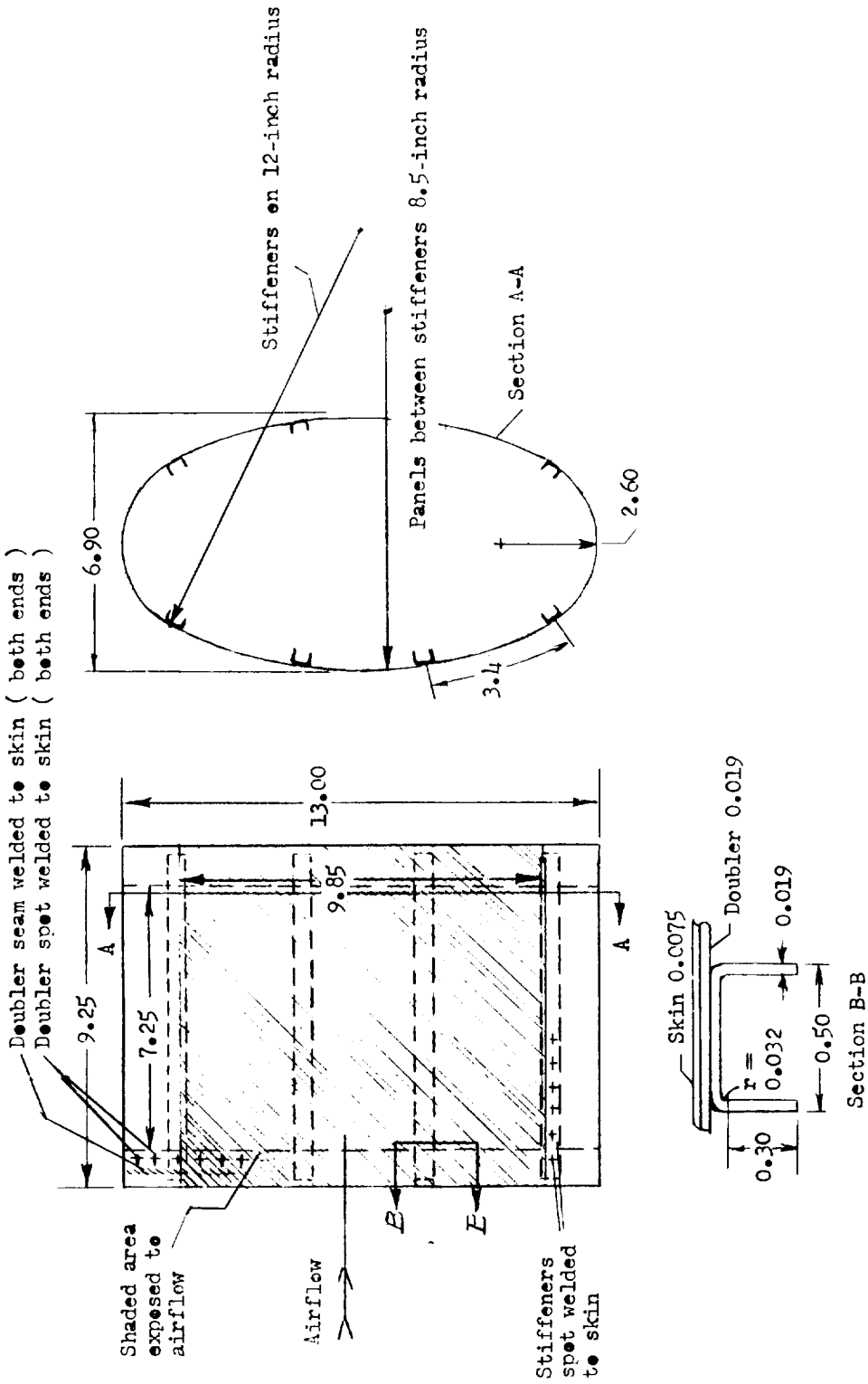

Figure 1.- Sketch of curved panel showing construction details.

L-61-1652.1

Figure 2.- Photograph of front of curved-panel model in test section of tunnel.

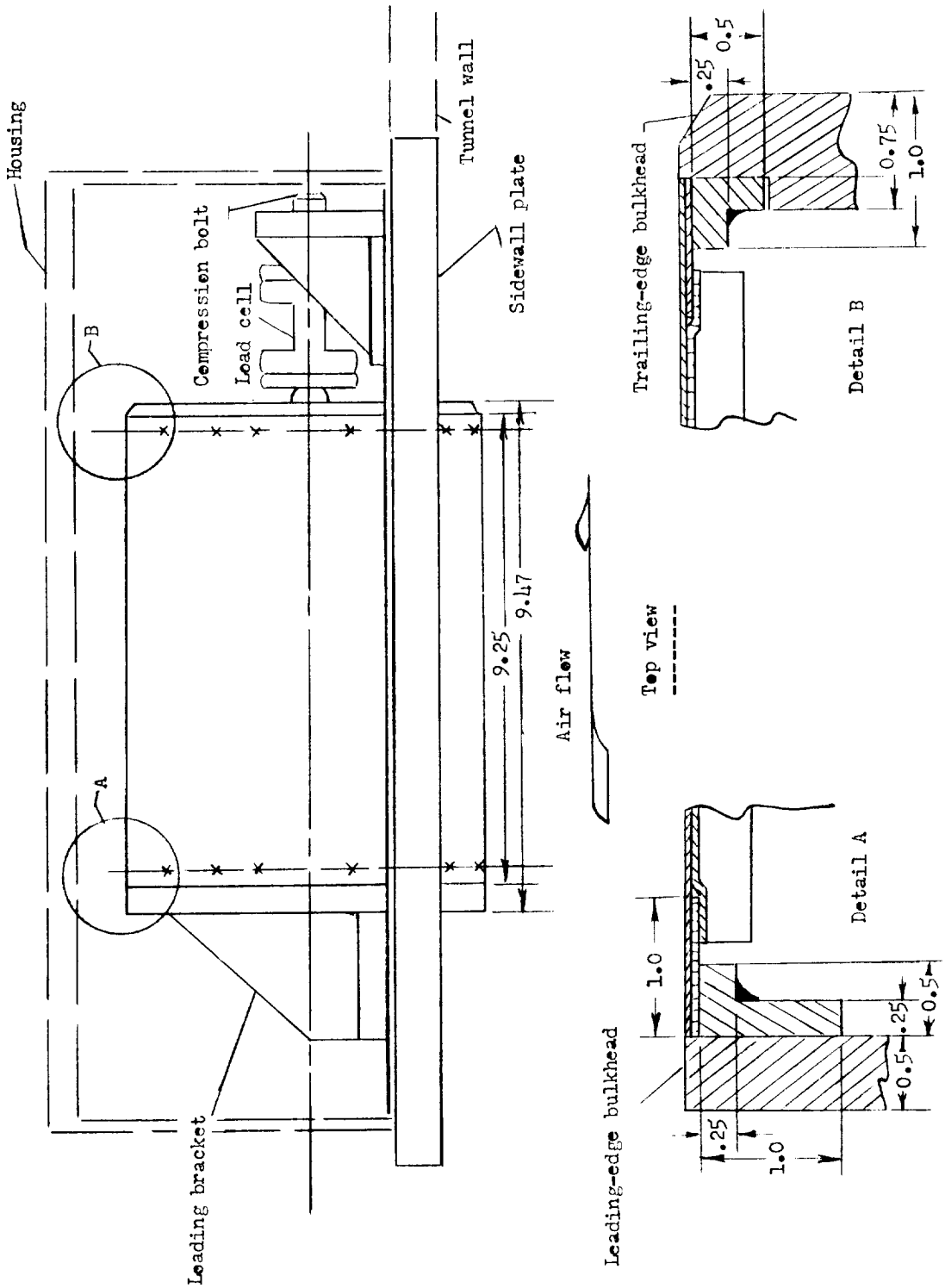

Figure 3.- Sketch of curved-panel support system.

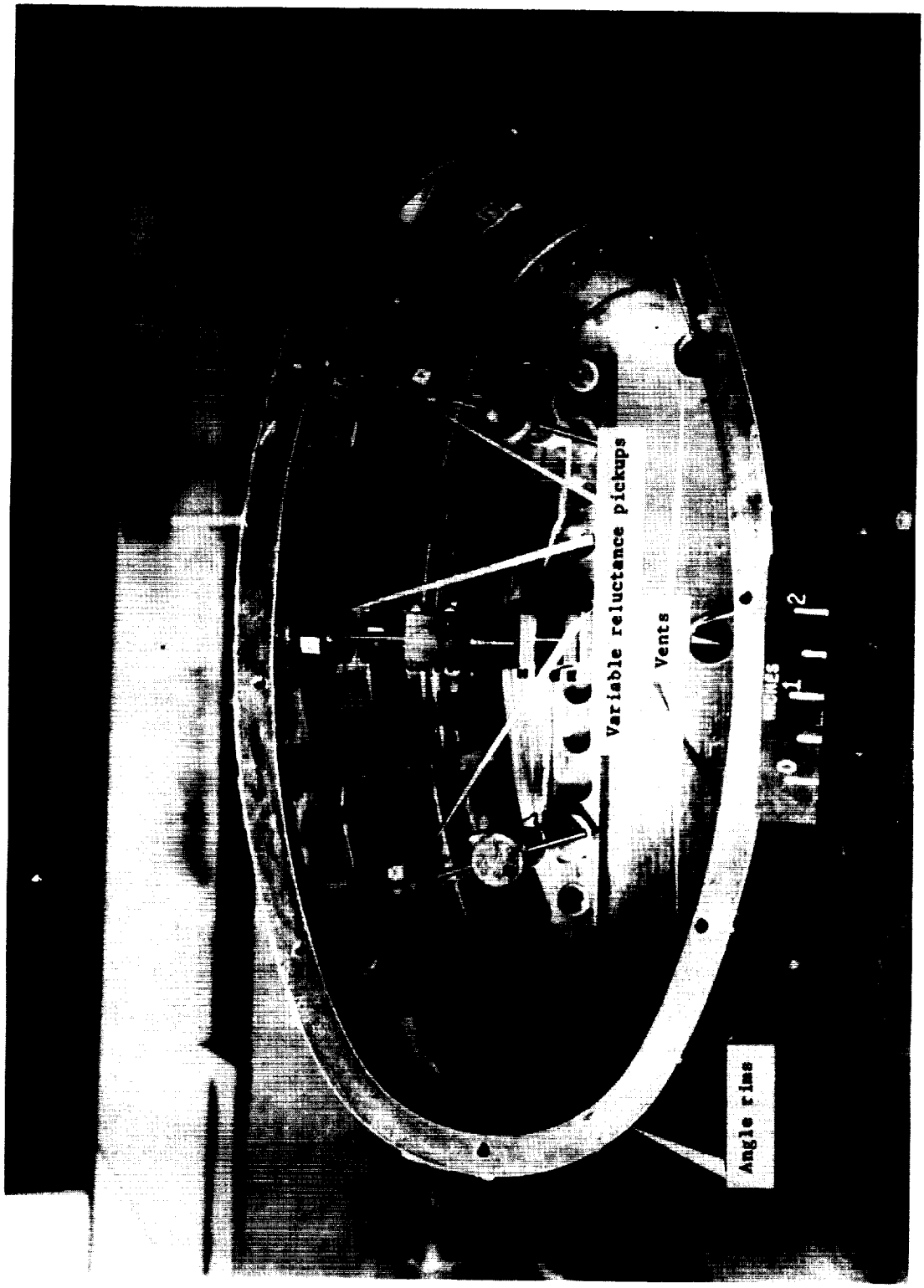

Figure 4.- Photograph of inside of curved-panel model. L-61-1650.1

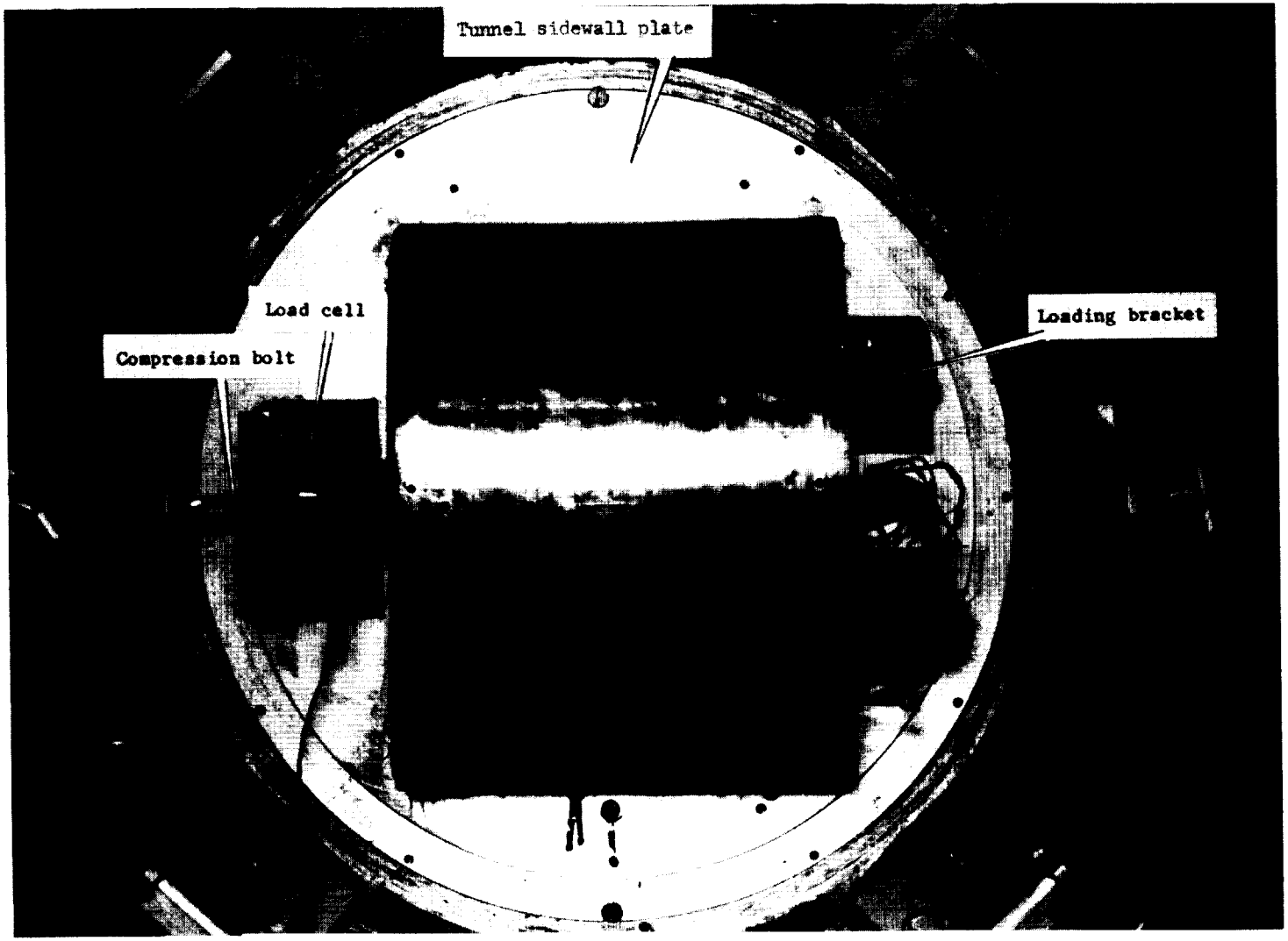

Figure 5.- Photograph of the back of the curved-panel model. L-61-1651.1

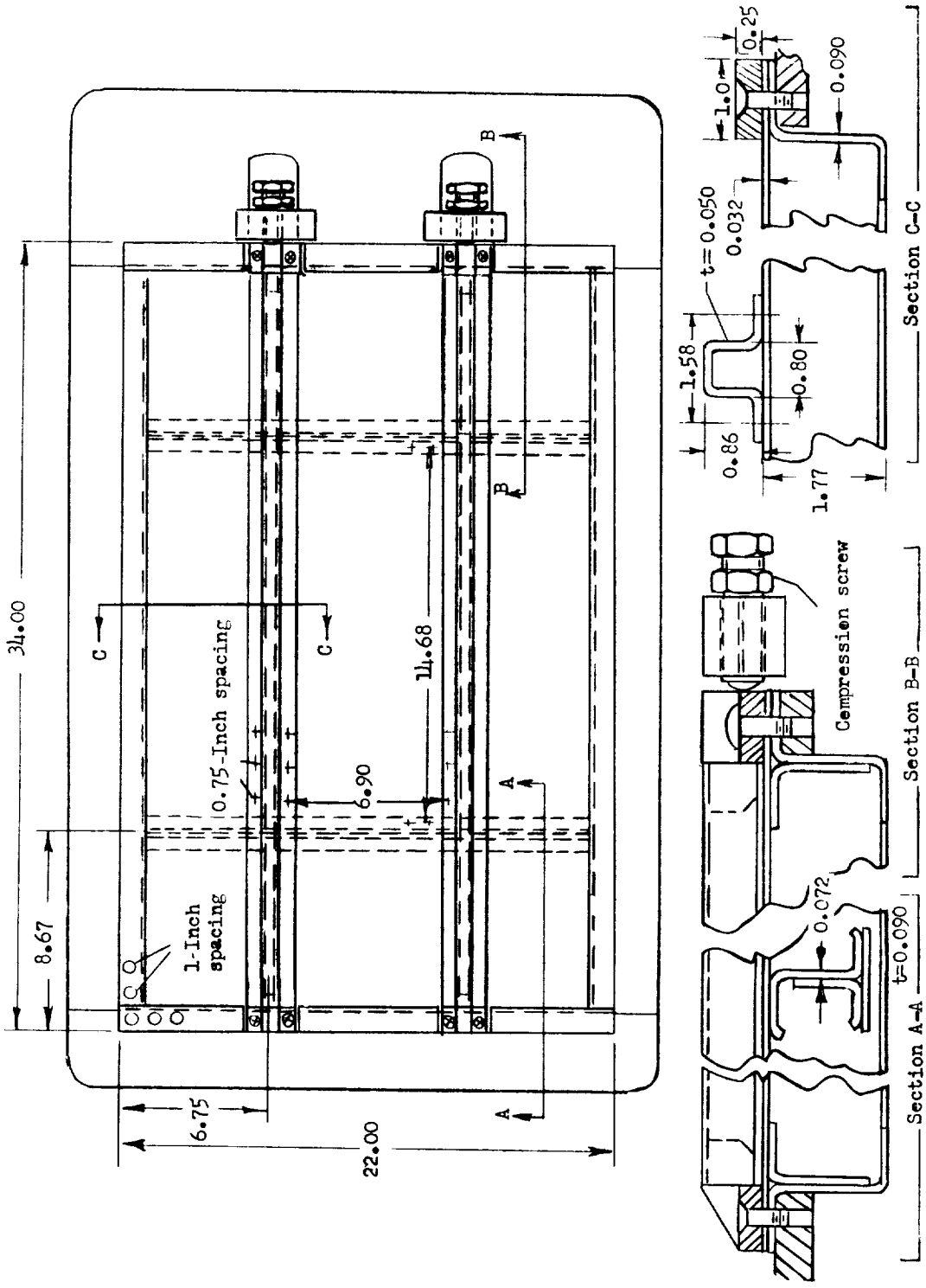

Figure 6.- Construction details of the flat panel.

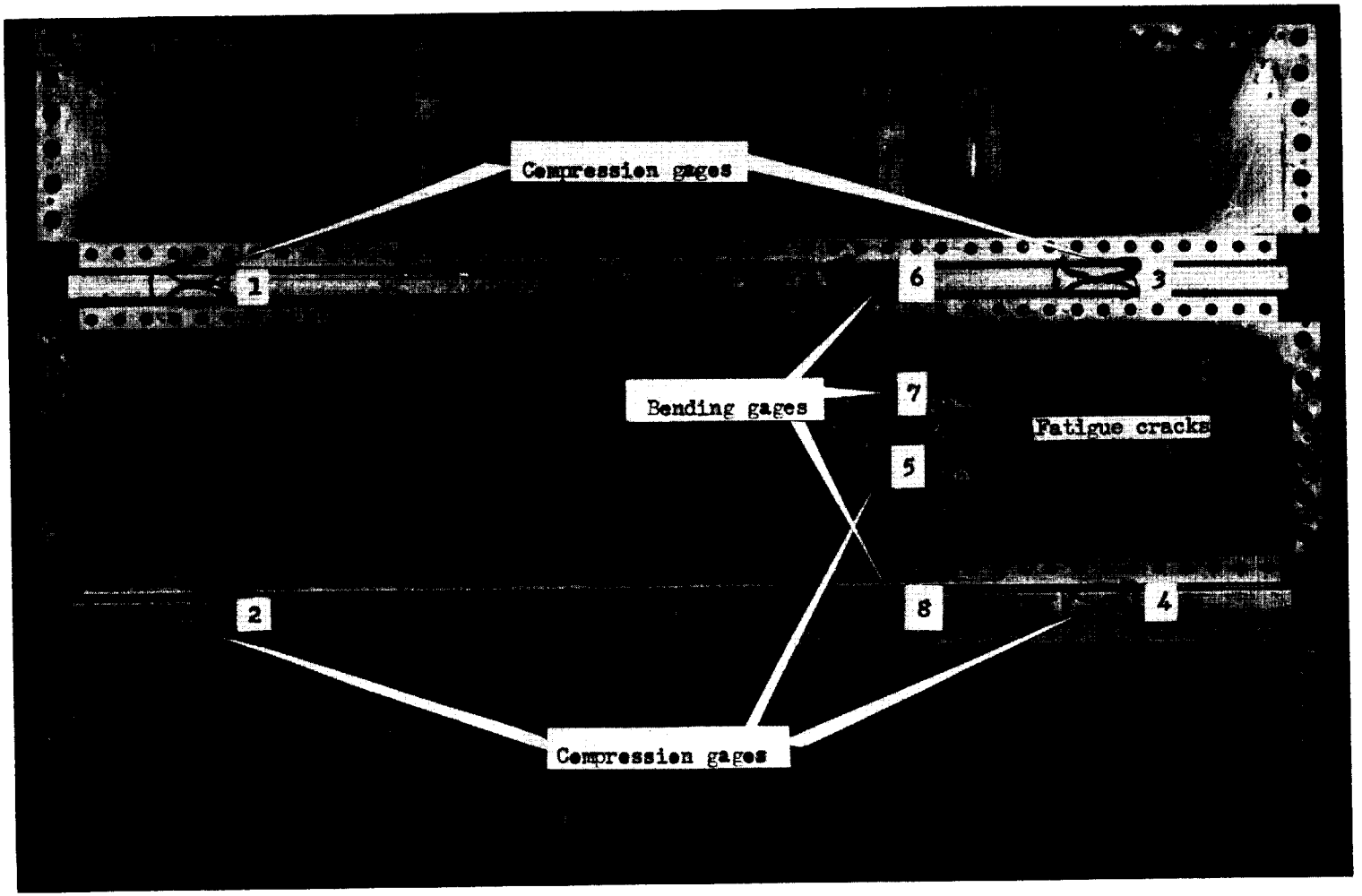

L-61-2870.1

Figure 7.- Photograph of front of flat panel showing fatigue cracks and strain-gage locations.

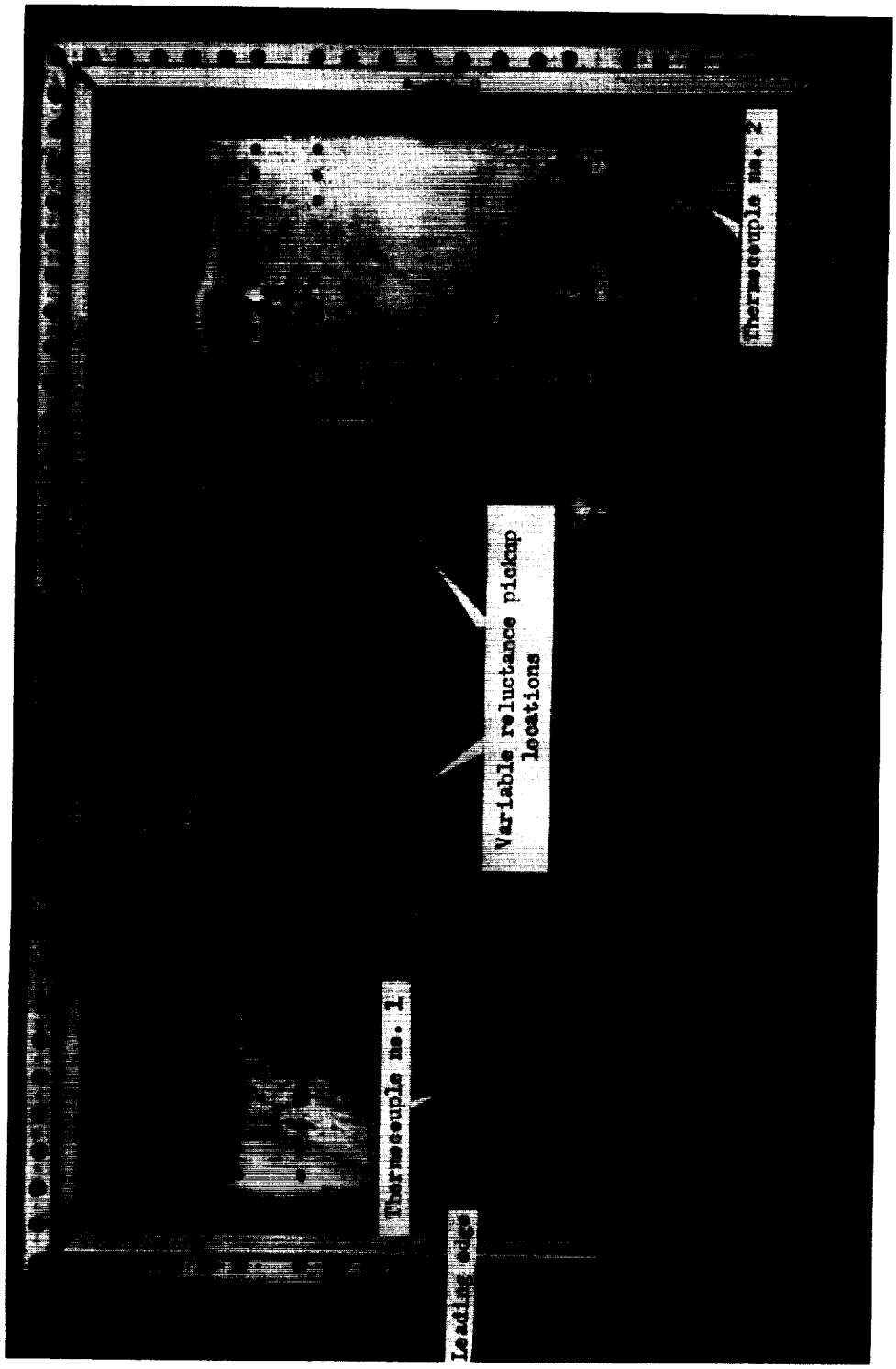

L-61-2871.1

Figure 8.- Photograph of back of flat-panel model showing locations of variable reluctance pickups and thermocouples.

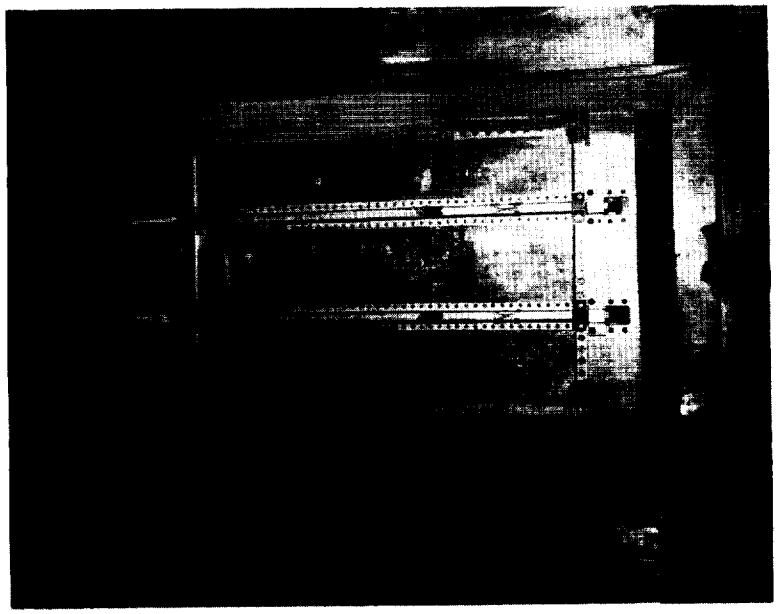

(a) Stringer fairings (runs 1 to 6). L-61-3008

(b) Wedge (run 7). L-61-3009.1

Figure 9.- Photograph of flat-panel model mounted on splitter plate with stringer fairings and with wedge.

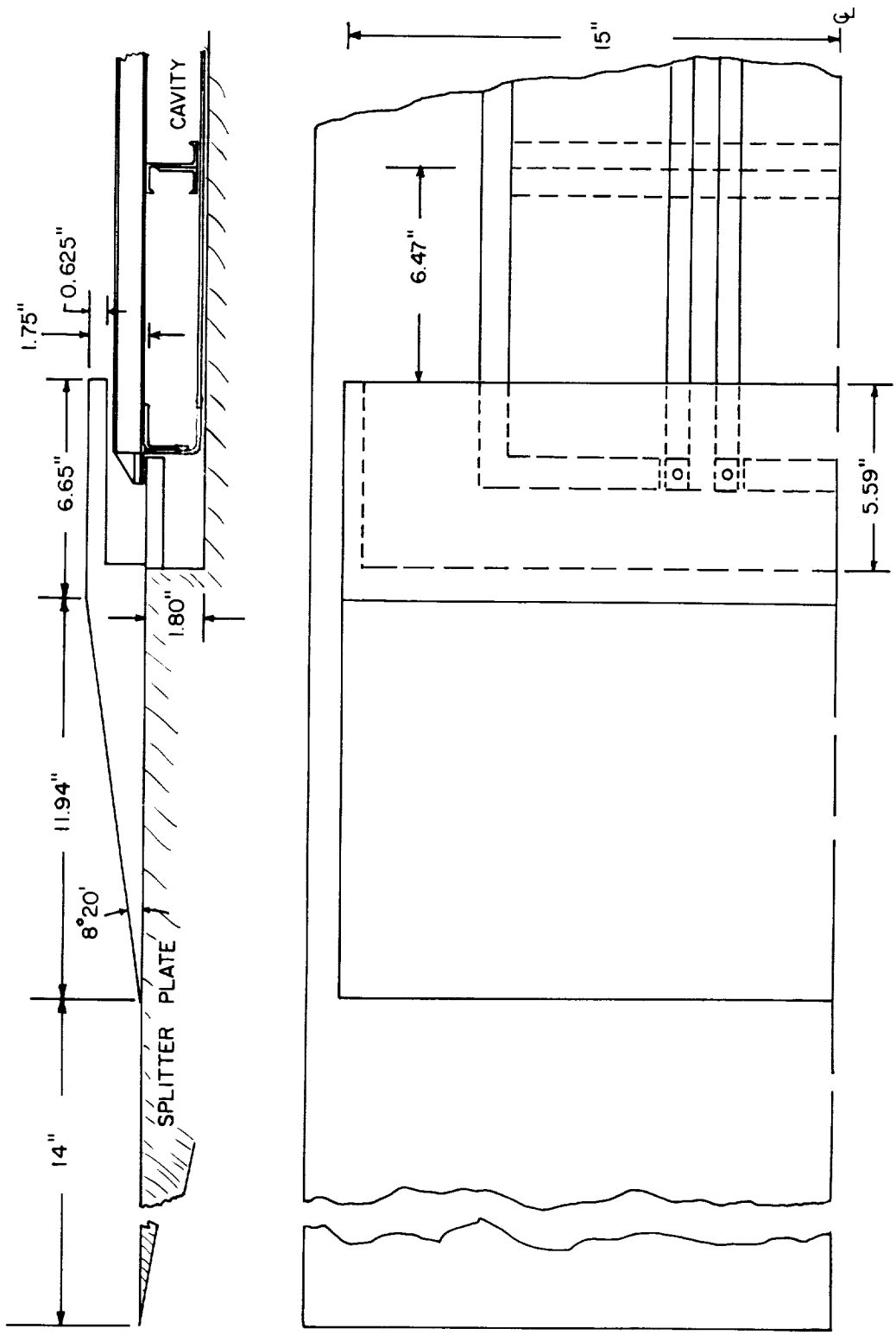

Figure 10.- Location of wedge with respect to the test panel (run 7).

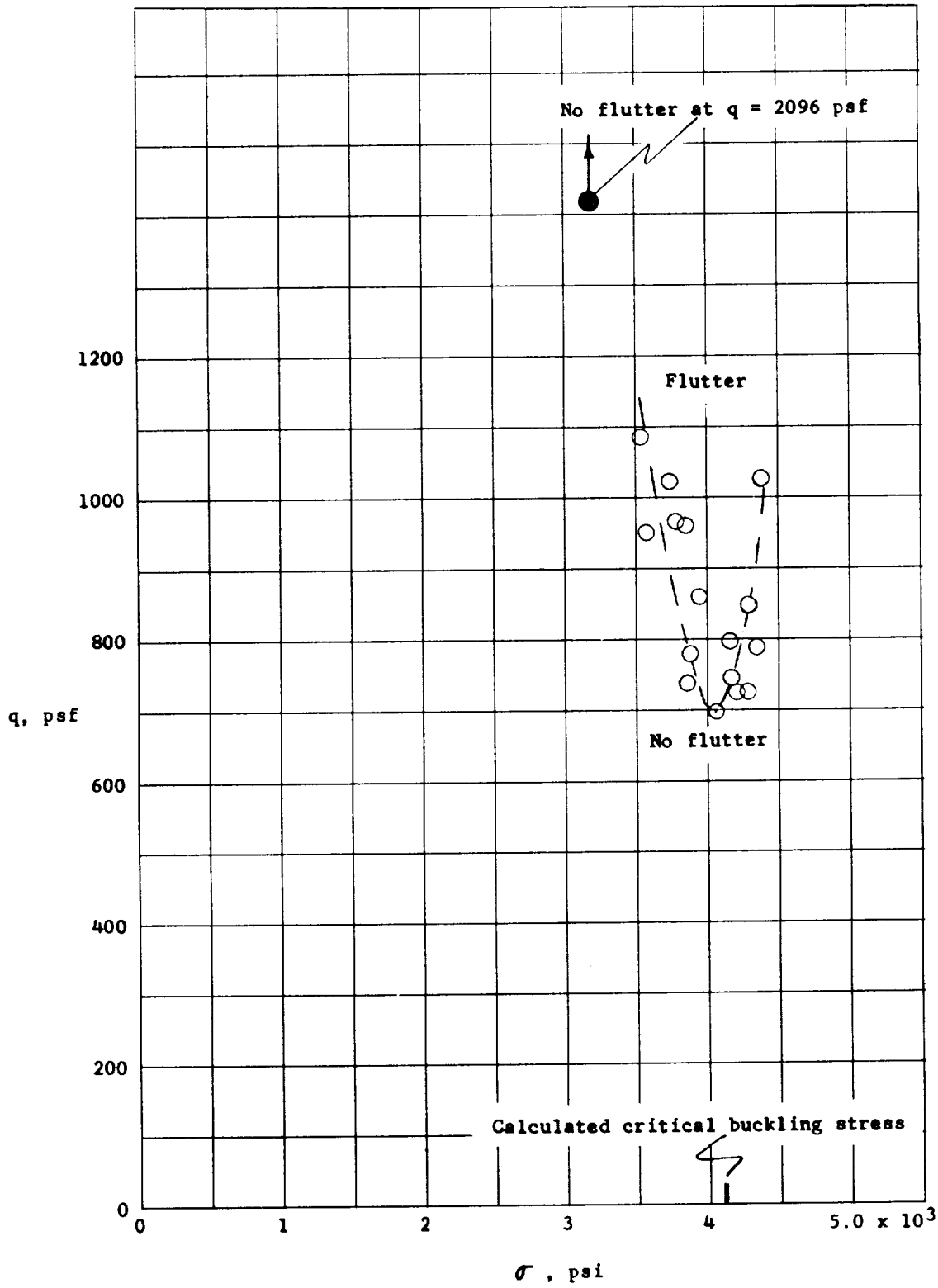

Figure 11.- Curved-panel test results. Dynamic pressure as a function of compressive stress at flutter. M = 1.97.

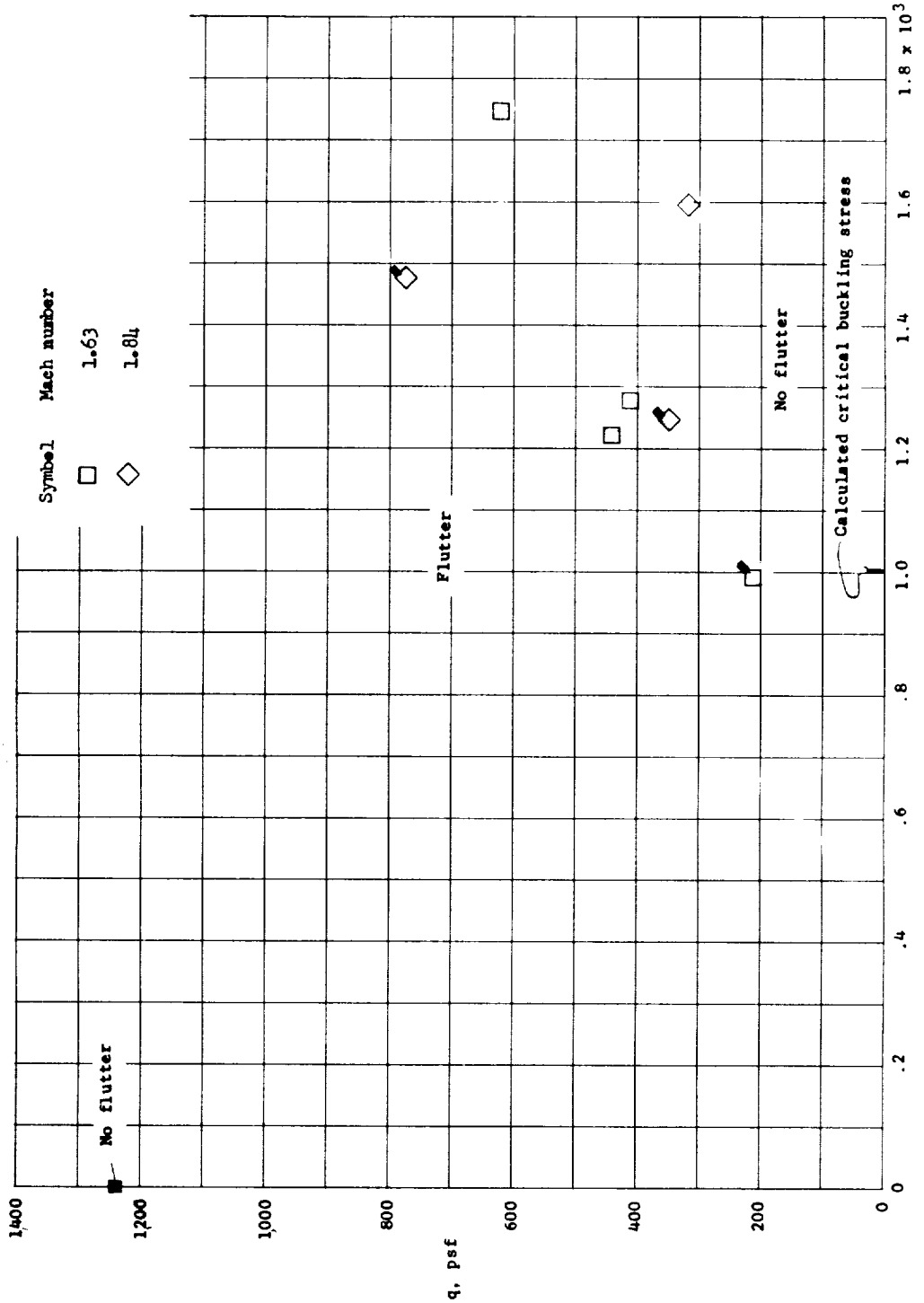

Figure 12.- Flat-panel test results. Dynamic pressure as a function of compressive stress in skin at flutter. Flagged symbols denote that the stresses were estimated.

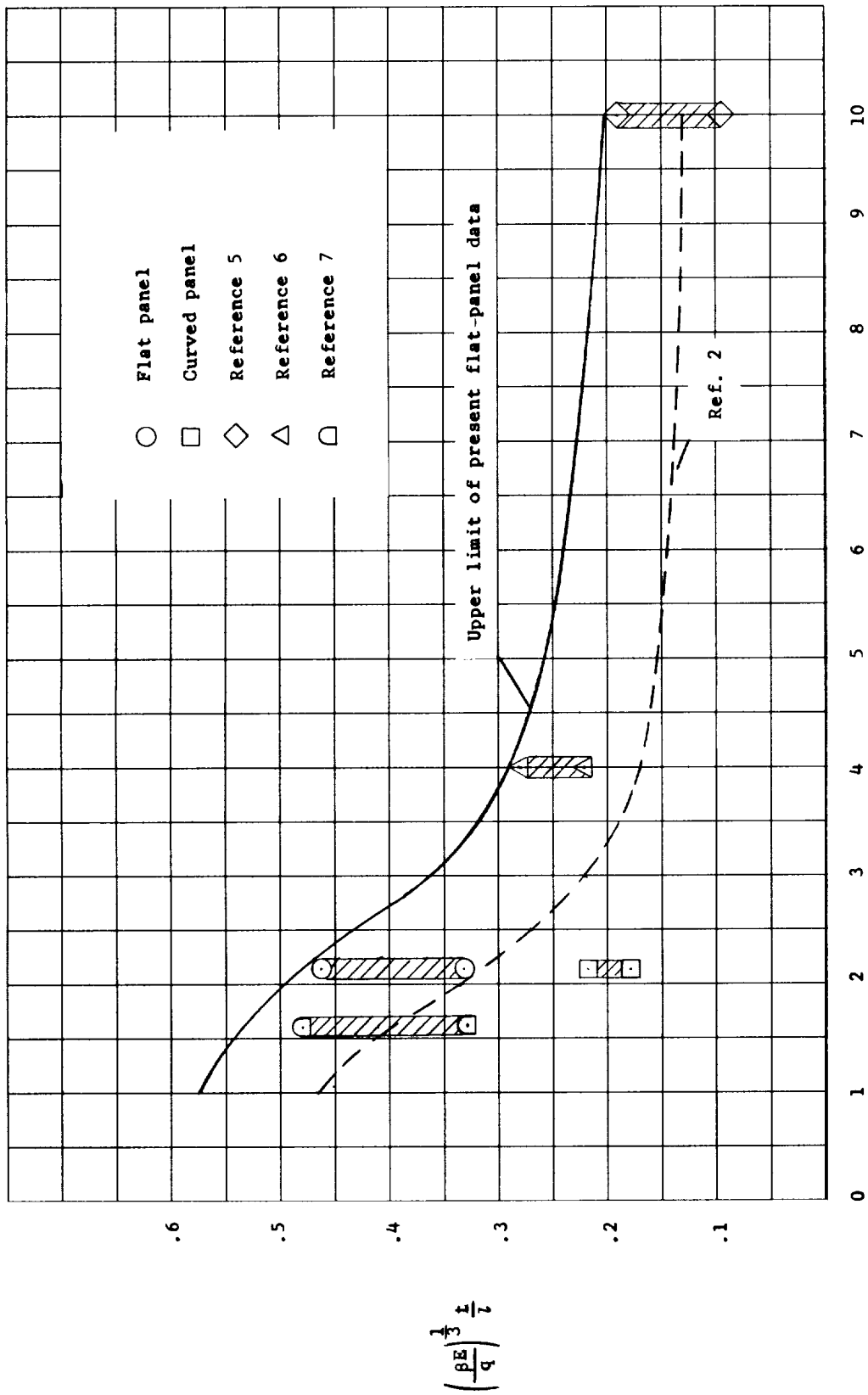

Figure 13.- Curved- and flat-panel flutter results as a function of the flutter parameter and the length-width ratio.

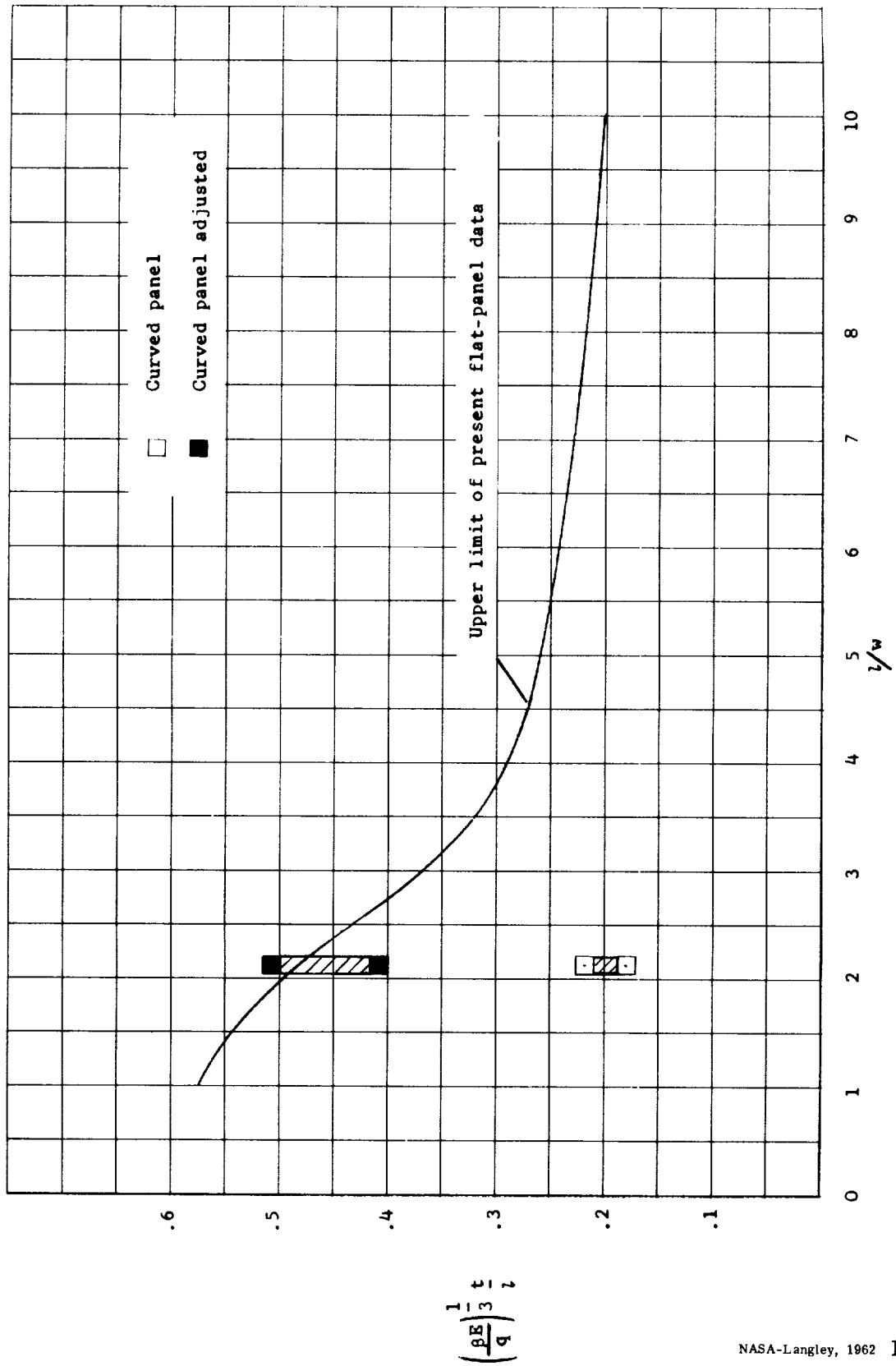

Figure 14.- The effects of curvature and the use of the critical buckling stress to adjust curved-panel test results.

NASA-Langley, 1962 L-2062